Radiochim. Acta **98**, 667–673 (2010) / **DOI** 10.1524/ract.2010.1767

Chlorine speciation in nuclear graphite: consequences on temperature release and on leaching

By C.-E. Vaudey[1], N. Toulhoat[1,2,*], N. Moncoffre[1] and N. Bérerd[1,3]

[1] Université de Lyon, Université Lyon 1, CNRS/IN2P3, UMR5828, Institut de Physique Nucléaire de Lyon (IPNL), 4 rue Enrico Fermi, 69622 Villeurbanne Cedex, France
[2] Commissariat à l'Energie Atomique CEA/DEN, Centre de Saclay, 91191 Gif sur Yvette Cedex, France
[3] Université de Lyon, UCBL-IUT Lyon 1, Département Chimie, 43 Bd. du 11 Novembre 1918, 69622 Villeurbanne Cedex, France

(Received September 28, 2009; accepted in revised form March 10, 2010)

^{36}Cl / *Nuclear graphite / Speciation / Temperature-programmed desorption / X-ray photoelectron spectroscopy / Disposal*

Summary. This paper aims to get information on pristine chlorine speciation and its evolution with temperature in nuclear graphite used as a moderator in the first generation UNGG French reactors. For this purpose, temperature-programmed desorption (TPD) and X-ray photoelectron spectroscopy (XPS) have been carried out on samples annealed in the temperature range 200–1000 °C. Two chemical forms of different thermal stabilities have been identified. Around 70% of chlorine is assigned to stable organic chlorine bound to aromatic carbon whereas around 30% is assigned to inorganic thermally labile oxychlorinated groups. The consequences for direct disposal are discussed.

1. Introduction

The dismantling of the first generation *Uranium Naturel Graphite Gaz* French reactors, called UNGG, will produce an important quantity of irradiated graphite waste. According to the French law of June 2006, a specific disposal must be created for this low activity waste. It is therefore necessary to assess the graphite waste long-term behaviour.

Nuclear graphite is manufactured from petroleum coke grains (filler) blended with coal tar pitch acting as a binder. Shaped blocks are formed by extrusion of the blend. They are heat-treated up to about 2800 °C (graphitisation treatment) and polycrystalline graphite is obtained. Blocks, intended for the moderator or reflector, may be further impregnated with pitch, re-baked and regraphitised in order to increase the density. Virgin nuclear graphites have initial densities in the range 1.6–1.8 g cm^{-3}. The difference with graphite crystal (density = 2.265 g cm^{-3}) is due to internal porosity [1]. As a result of mixing of several carbon compounds, this material is structurally heterogeneous at a local scale. Nuclear graphite presents a complex multiscale organisation. It can be locally more or less anisotropic and not completely graphitised. Nuclear graphite has a polycrystalline structure and contains micrometer sized grains. The grains are formed by several more or less oriented crystallites with a size of a few hundreds nanometers. Each crystallite is formed by a triperiodical stacking of graphene planes. Nuclear graphite contains also small amounts of impurities like oxygen, hydrogen, metals and halogens, among them chlorine. Chlorine contents range from some at. ppm to around 50 at ppm (called pristine chlorine in the following). It could result from graphite purification (elimination of sulphur and metallic impurities) [2], as well as be present as an impurity in coke or pitch.

During reactor operation, the main part of ^{35}Cl is activated into ^{36}Cl [3, 4]. Consequently, irradiated nuclear graphite contains ^{36}Cl isotope as an impurity. ^{36}Cl has a long radioactive half-life (about 300 000 years) and, depending on its chemical form, can be highly soluble in water and mobile in the environment. ^{36}Cl can be released during dismantling and storage. Moreover in the case of long term disposal, it may contribute to a significant dose peak at the outlet after water ingress into the site [5]. The release of ^{36}Cl could have an impact on environment because of the high soil to plant transfer factor of chlorine [6, 7]. The release of ^{36}Cl depends on different processes such as water saturation or water access into graphite pore spaces. Moreover, the solubilisation of ^{36}Cl is controlled by its chemical form, as well as its properties regarding diffusion and retention. In order to be able to identify and quantify the release mechanisms of ^{36}Cl into water, it is necessary to determine its location and speciation before any contact between graphite and water *i.e.* before dismantling and disposal.

During reactor operation, two main factors determine chlorine's behaviour: temperature and corrosion (thermal or radiolytic) [8]. A previous paper was focused on the thermal behaviour of implanted chlorine used to simulate ^{36}Cl displaced from its original structural site by recoil during reactor operation. It was shown that around 20% of chlorine is almost athermally released after 4 h at 500 °C (mean temperature during reactor operation), mainly through open pores (activation energy $E_a < 0.1$ eV) [9]. For longer annealing durations (over 10 h) and higher temperatures such as 800 °C, the loss of chlorine reaches a plateau. Our results were in agreement with those of Clayton *et al.* [10] obtained

*Author for correspondence (E-mail: n.toulhoat@ipnl.in2p3.fr).
Present address: IPNL, Bâtiment Dirac, 4 rue Enrico Fermi, 69622 Villeurbanne Cedex, France

on irradiated graphite. These authors measured a rapid release of around 50% of the initial chlorine in Magnox and 30% in advanced graphite reactors (AGR). Moreover, they suggest that further 40% of the remaining chlorine is released over the reactor lifetime. All these results point towards the existence of two chlorine chemical forms of different thermal stabilities. It is likely that during reactor operation the more labile fraction is rapidly released.

This paper aims to get more insight in the thermal behaviour of pristine chlorine in nuclear graphite by 1) investigating the chemical forms of the desorbed chlorine species using temperature-programmed desorption (TPD) and thermogravimetry (TG) and 2) identifying the chemical forms and speciation of chlorine in virgin nuclear graphite using X-ray photoelectron spectroscopy (XPS).

2. Experimental

2.1 Samples

Several samples of virgin nuclear graphite (pile grade) used in the French nuclear reactor Saint Laurent A2 (graphite moderated and CO_2 cooled reactor) have been studied (Fig. 1). Two kinds of samples have been investigated. Both have been cut in a same block (Fig. 1a). The first one, called XY, contains grains preferentially oriented perpendicularly to the spinning axis. The second one, called Z, contains grains preferentially oriented along to the spinning axis. As a consequence, the XY sample contains more inter crystallite pores than the Z sample (Fig. 1b).

2.2 Analysis

2.2.1 Characterisation of desorbed species from nuclear graphite

TPD experiments have been carried out in secondary vacuum, between room temperature and 800 °C with a ramp of 20 °C min^{-1}. The desorbed gases have been analysed on line by mass spectrometry, using a Balzers instrument QMG 112, at the "Ecole Nationale Supérieure des Mines de St Etienne" (ENSM-SE, France).

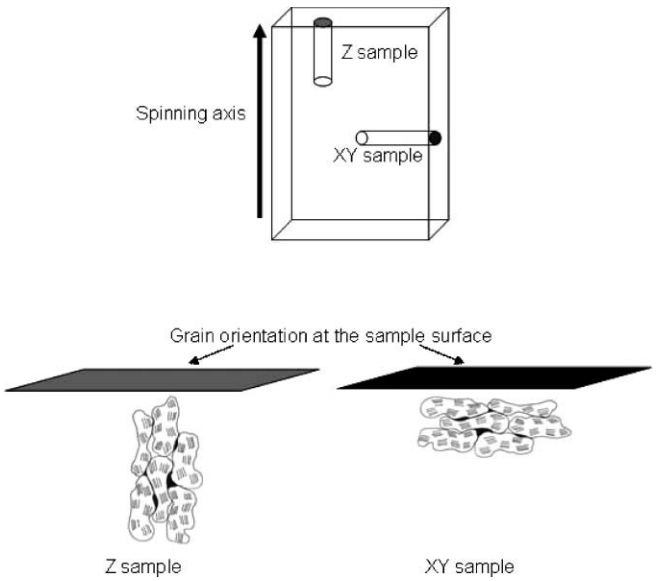

Fig. 1. (**a**) Sketch of XY and Z samples cut in a block of St Laurent A2 nuclear graphite, (**b**) sketch of the grain orientation at the XY and Z sample surfaces.

2.2.2 Evolution of nuclear graphite density and mass during thermal treatment

In order to control the nuclear graphite density, helium pycnometry measurements have been carried out before and after TPD. Moreover, the nuclear graphite sample mass has been monitored by TG. The analyses have been performed, under nitrogen atmosphere with a flux of 100 mL min^{-1}, for temperatures ranging between 25 and 1000 °C, and a ramp of 10 °C min^{-1}, using a TA Instruments 2950 HR V5.3.

2.2.3 Carbon and chlorine speciation

The carbon and chlorine chemical forms have been identified in virgin and annealed graphite samples using the XPS technique with a PHI Quantera SXM. A monochromatic Al K_α source with the X-ray power set at 50 W has been used. The binding energies have been referenced to the Fermi level of the electron analyser and the binding energies scale has been calibrated against Au 4 $f_{7/2}$ and Cu 2 $p_{3/2}$ at 83.96 eV and 932.62 eV respectively. The accuracy on the peak positions is equal to ±0.2 eV. To suppress the influence of an eventual atmospheric contamination, the analyses have been performed on fresh sample surfaces cleaved under vacuum. In our case, the detection limit is around 40 at ppm. According to [11], the quantification limit should be around 0.01 at. %. As the chlorine contents of our samples are just above the detection limit, it is impossible to quantify the data. Therefore, in order to compare the different samples, we chose to compare the peak areas. The accuracies on the peak areas are in the range of 2 to 5% depending on the element content in the sample. The values are therefore of 2% for the C 1*s* peak and of 4.4% for the Cl 2*p* peak in virgin samples. In order to check the reproducibility of the data, we performed multiple analyses on the same sample. The calculated uncertainties take into account this reproducibility. They have been estimated to be 4% for the C 1*s* peak and 9% for the Cl 2*p* peak in virgin samples.

3. Results and discussion

3.1 Characterisation of desorbed species from nuclear graphite

Fig. 2 represents the nature and quantity of desorbed gases as a function of temperature for both sample orientations. The main gases are carbon monoxide, carbon dioxide, water, nitrogen dioxide, oxygen and hydrogen chloride (respectively Fig. 2a–f). Except HCl, the gases are all oxygenated gases, which correspond probably to the removal of chemisorbed or physisorbed oxygen compounds. According to Polovina *et al.* [12], the chemisorbed oxygen begins desorbing at around 200 °C. Pristine chlorine desorbs as HCl and no Cl_2 has been detected. For all gases, the desorption behaviour confirms the texture influence. Indeed, as sample XY contains more pores, the gases start desorbing at lower

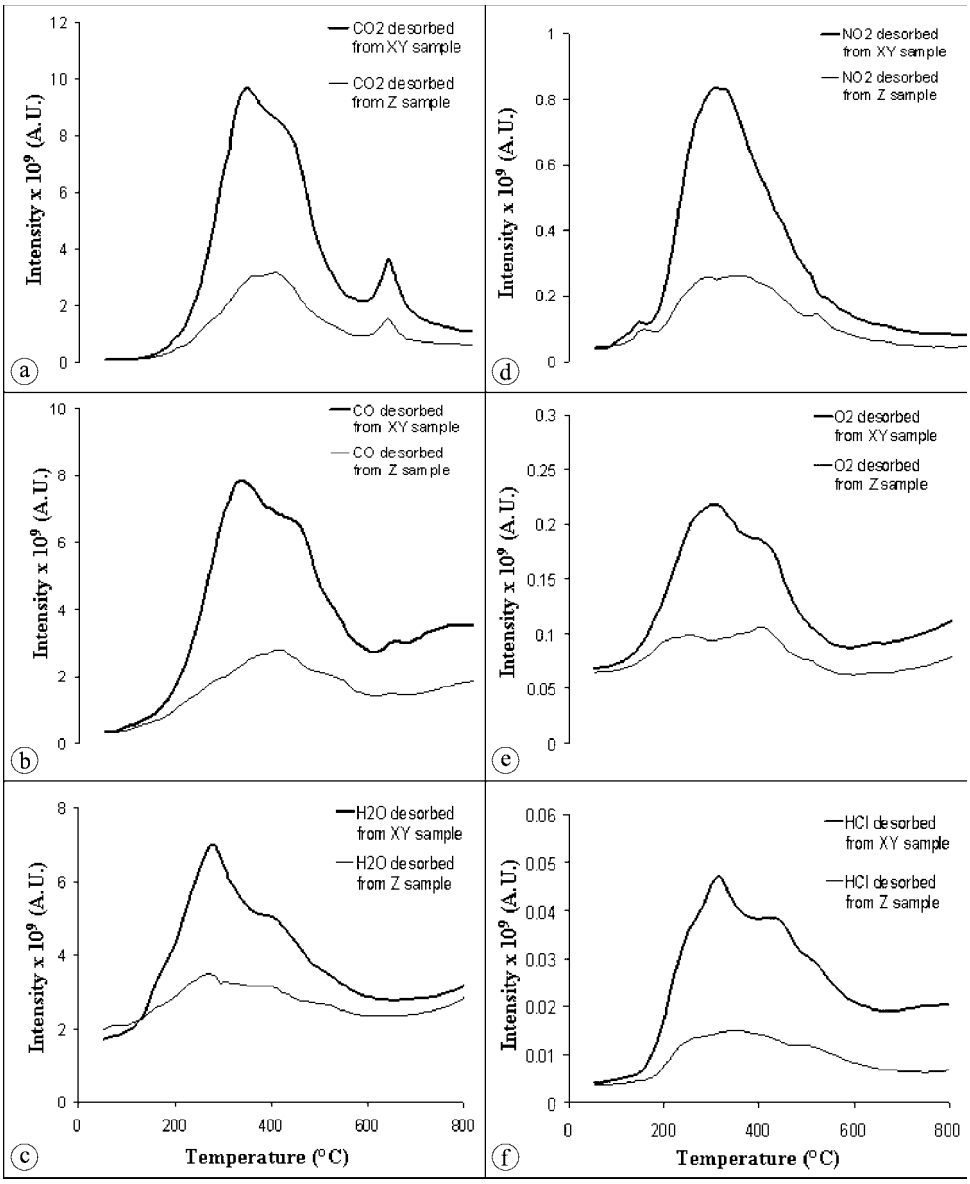

Fig. 2. Quantities of (**a**) carbon dioxide, (**b**) carbon monoxide, (**c**) water, (**d**) nitrogen oxide, (**e**) oxygen and (**f**) hydrogen chloride desorbed from virgin nuclear graphite for XY and Z samples monitored by TPD.

temperatures compared to the sample Z, the pores forming preferential release paths. This result is in agreement with previous results presented in [9].

For each sample, the desorbed quantity of hydrogen chloride is 150 times lower than that of carbon monoxide or carbon dioxide. The hydrogen chloride desorption (Fig. 2f) occurs between 200 and 600 °C and results in a peak around 350 °C followed by a shoulder around 450 °C. This desorption in two steps is also observed for the oxygenated gases. This desorption dynamics could reflect the presence of two locations with different accessibilities. Concerning chlorine, it could also put in evidence the existence of two chemical forms. Similar results have been obtained by Takeda *et al.* [13] for HCl in coal. The authors interpreted the two contributions as a signature of two chemical forms of chlorine.

3.2 Evolution of the nuclear graphite density and mass during thermal treatment

The sample density has been measured before and after TPD. A decrease of the sample density (ratio mass/volume) has been induced by the thermal treatment (respectively $2.12 \pm 0.02\ \mathrm{g\,cm^{-3}}$ before TPD and $1.91 \pm 0.02\ \mathrm{g\,cm^{-3}}$ after). This result has been confirmed by TG analysis. A decrease of the sample mass smaller than 1% has been measured. This implies that, under thermal treatment between room temperature and 1000 °C and in nitrogen or in argon atmosphere, the corrosion of graphite is negligible.

3.3 Carbon and chlorine speciation

In order to identify the chemical forms of carbon and chlorine, we have focused our experiments on the C 1*s* peak (Fig. 3) and on the Cl 2*p* peak (Fig. 4). The analyses have been performed on the surfaces of two virgin St Laurent A2 samples cleaved under vacuum. A good reproducibility of the results has been observed. The analyses have also been performed on samples annealed (under argon atmosphere) at 200, 600 and 1000 °C.

3.3.1 Carbon speciation

Fig. 3a displays the XPS spectrum of the carbon 1*s* peak obtained on virgin graphite. The carbon 1*s* peak is characteristic of carbonaceous materials. The main peak, located

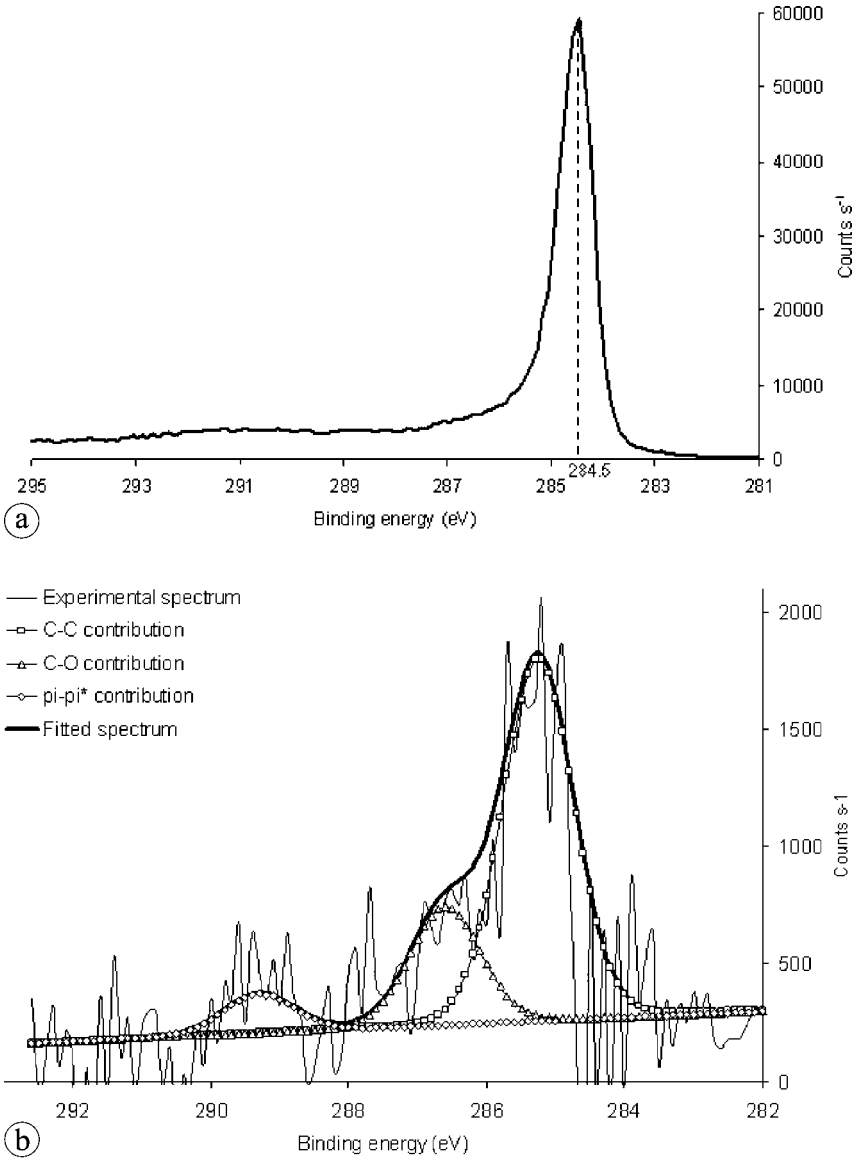

Fig. 3. XPS spectra (experimental and fitted): (**a**) carbon 1*s* peak of St Laurent A2 virgin nuclear graphite and (**b**) spectrum resulting from the subtraction of the C 1*s* peak measured at 1000 °C from the one measured at 200 °C.

at 284.6 ± 0.2 eV, corresponds to the contribution of aromatic layer in graphitic sp^2 configuration. This peak has a dissymmetric shape and its broadening at higher energies is related to the neutralisation, by conduction electrons, of the holes created during the photoionisation. This dissymmetric peak is known to be representative of pure graphite material [14–16]. A second contribution, shifted to higher energies (around 5 at 6 eV) and situated between 290 and 292 eV, is due to the π–π^* shake-up satellite [14]. We can note that the high base line at the left of the main peak, around 286.5 eV, is in favour of the presence of carbon atoms covalently bound to oxygen atoms [14, 17, 18].

In order to remove the main sp^2 contribution from the carbon 1*s* peak, the spectrum obtained at 1000 °C has been subtracted from the one obtained at 200 °C. The resulting spectrum is presented in Fig. 3b. This procedure allows focusing on the other contributions and evaluating the evolution of carbon speciation during thermal treatment. The resulting peak has been fitted to three contributions (Table 1). These different binding energy peaks have been assigned to C−C at 285.4 ± 0.2 eV (covalent bounds between sp^3 carbon atoms [17]), C−O at 286.5 ± 0.2 eV (carbon atoms covalently bound to oxygen atoms [14, 17, 18]) and to π–π^* levels transition at 289.5 ± 0.2 eV [14]. The respective relative areas are 59 ± 4, 21 ± 4 and 20 ± 4%. The accuracies on the C 1*s* peak areas take into account the uncertainties resulting from the fitting procedure and the multiple analyses. From the values of these relative areas it can be inferred that, a temperature increase from 200 °C to 1000 °C induces a decrease of the C−C contribution corresponding to a progressive removal of sp^3 carbons. As well, these values indicate a break of covalent bonds, such as C−O,

Table 1. Nature of the contributions, binding energies and relative areas for the peak resulting from the subtraction of the spectrum measured by XPS at 1000 °C from the one measured at 200 °C.

Nature of the contribution	Binding energy (eV)	Relative area (%)
C−C	285.4 ± 0.2	59 ± 4
C−O	286.5 ± 0.2	21 ± 4
π–π^*	289.5 ± 0.2	20 ± 4

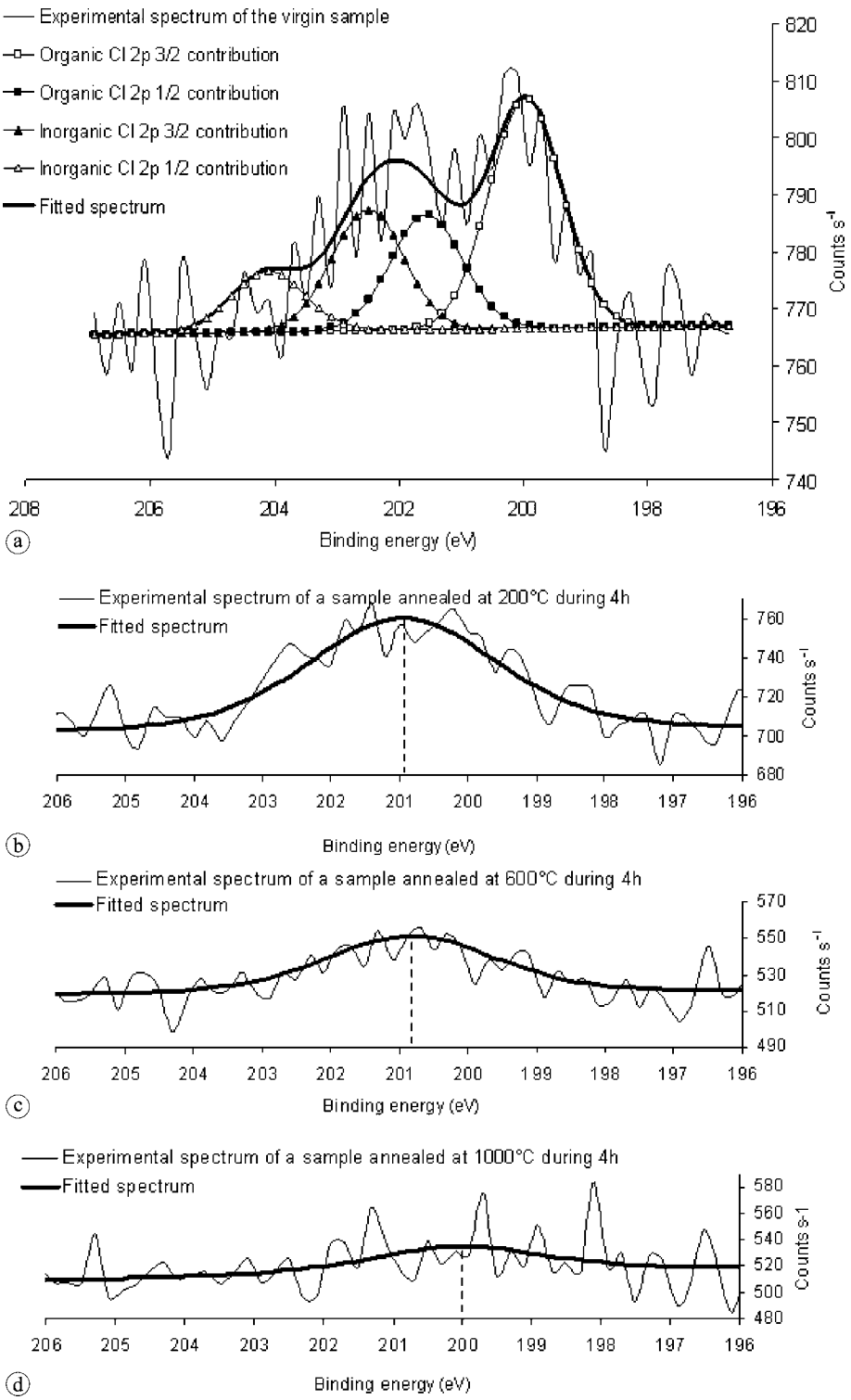

Fig. 4. XPS spectra of the chlorine 2*p* peak of St Laurent A2 nuclear graphite: (**a**) virgin and annealed (**b**) 4 h at 200 °C, (**c**) 4 h at 600 °C and (**d**) 4 h at 1000 °C.

corresponding to the release of oxygenated groups from the sample.

3.3.2 Chlorine speciation

Fig. 4 displays the XPS spectrum of the chlorine 2*p* peak obtained in virgin graphite. The fitting of this peak results in two contributions whose characteristics are presented in Table 2. The contribution, centred at 200.0 ± 0.2 eV, corresponds to organic chlorine. The other one, centred at 202.5 ± 0.2 eV, is due to inorganic chlorine [19]. The comparison of

Table 2. Nature of the contributions, binding energies and relative areas for the fitted Cl 2*p* peak measured by XPS on the virgin graphite.

Nature of the contribution		Binding energy (eV)		Relative area (%)	
Organic chlorine	$2p_{3/2}$	200.0 ± 0.2	199.9 ± 0.2	70 ± 9	46 ± 9
	$2p_{1/2}$		201.6 ± 0.2		24 ± 9
Inorganic chlorine	$2p_{3/2}$	202.5 ± 0.2	202.5 ± 0.2	30 ± 9	21 ± 9
	$2p_{1/2}$		204.1 ± 0.2		11 ± 9

Table 3. Evolution of the XPS Cl $2p$ peak (binding energies and areas) measured by XPS on St Laurent A2 virgin samples before and after thermal annealing.

Sample	Binding energy (eV)	Cl $2p$ peak area (number of counts s^{-1})
Virgin	200.0 ± 0.2 and 202.5 ± 0.2	115 ± 5
Annealed 200 °C 4 h	200.9 ± 0.2	81 ± 12
Annealed 600 °C 4 h	200.7 ± 0.2	62 ± 14
Annealed 1000 °C 4 h	200.0 ± 0.2	< 30

the respective relative peak areas corresponding to organic ($2p_{3/2} + 2p_{1/2}$) and inorganic ($2p_{3/2} + 2p_{1/2}$) chlorine shows that, in virgin graphite $70 \pm 9\%$ is organic and $30 \pm 9\%$ inorganic. The accuracies take into account the uncertainties resulting from the fitting procedure and the multiple analyses.

The organic chlorine corresponds to C−Cl (chlorine atoms covalently bound to sp^2 carbon of aromatic rings) [20–22]. The chlorine atoms have been substituted to some hydrogen atoms during the purification stage of graphite manufacturing [23, 24]. The organic chlorine contribution is composed of two peaks situated at 199.9 ± 0.2 eV ($Cl_{organic}\ 2p_{3/2}$) and centered at 201.6 ± 0.2 eV ($Cl_{organic}\ 2p_{1/2}$) (Table 2). The binding energy difference of 1.6 ± 0.2 eV between both peaks is in good agreement with the literature, as well as the Cl $2p_{3/2}$/Cl $2p_{1/2}$ ratio of 2 [25].

The inorganic chlorine corresponds to oxychlorinated groups like ClO_2^- and ClO_3^- [20]. As for organic chlorine, two contributions have been assigned to $Cl_{inorganic}\ 2p_{3/2}$ at 202.5 ± 0.2 eV and $Cl_{inorganic}\ 2p_{1/2}$ at 204.1 ± 0.2 eV (Table 2). The binding energy difference and the ratio of the two relative areas are in agreement with the literature [25].

Table 3 displays the binding energy and the Cl $2p$ peak area for virgin and annealed samples. We observe a decrease of the peak areas corresponding to chlorine release as a function of temperature. Between 200 and 1000 °C, the evolution of the binding energies corresponds to a progressive decrease of the inorganic chlorine contribution. At 1000 °C, the inorganic chlorine contribution has totally disappeared [19]. This result shows that the chlorine compounds have different thermal stabilities: the more labile oxychlorinated groups, weakly bound to the graphite matrix, are released at lower temperature than the stable C−Cl groups. This result is in agreement with the oxygenated groups release observed previously (Fig. 3b).

3.4 Consequences for disposal

The aqueous leaching of chlorine in nuclear graphite will mainly depend on the impregnation kinetics, the chemical form and distribution patterns of chlorine in graphite, and the diffusion of the soluble species through its pores. ^{36}Cl leaching experiments, performed by Comte [26], Guy *et al.* [27] and Pichon [28], on irradiated nuclear graphite issued from the reactor G2, show that around 80% of ^{36}Cl is released during the first month (diffusion coefficient $D \approx 1 \times 10^{-11}$ m^2 s^{-1}) whereas a residual fraction is released with a much slower kinetics. According to these authors, this behaviour points towards the existence of two distinct chlorine types: a more labile fraction that is less bound to the graphite structure and another one which is more stable, more strongly bound to graphite and/or present in the infrapores. Our results are clearly in agreement with the findings of these authors concerning the existence of two types of chlorine. Indeed, our results point out the existence of an organic form of chlorine, strongly bound to graphite through C−Cl bounds resistant to leaching and an inorganic form, where chlorine is present as ClO_2^- or ClO_3^- compounds being far less resistant to leaching.

4. Conclusion

This paper aims to study the effects of temperature on the speciation of pristine chlorine in the Saint Laurent A2 French nuclear graphite. Using TPD in the temperature range 200–1000 °C and XPS, we have shown that: 1) chlorine is released as HCl; 2) two chlorine chemical forms are present in virgin graphite. They correspond respectively to:

– inorganic chlorine, around 30%, probably chlorite (ClO_2^-) and chlorate (ClO_3^-) compounds;
– organic chlorine, around 70%, aromatic carbon (C−Cl) bonds.

These compounds have different thermal stabilities: the release of inorganic compounds increase with temperature whereas the organic chlorine remains more stable.

This feature will determine ^{36}Cl's behaviour during dismantling and disposal as the chlorites and chlorates will be less resistant to leaching than carbon bound chlorine.

Complementary experiments are underway in order to take into account the effects of thermal and radiolytic corrosion on chlorine speciation and behaviour.

Acknowledgment. The authors would like to thank F. Bérenger (EDF CIDEN) and L. Petit (EDF R&D) for their support, M. Pijolat, from the ENSM-SE, who granted access to the TPD facility and C. Grossiord from "Science et Surface" for helpful discussions with XPS. This work is supported by the French program PACEN (PARIS) and by the European project CARBOWASTE.

References

1. IAEA TEC DOC 1521 (2006).
2. Cornuault, P.: *Génie Nucléaire, Modérateurs, Graphite*. 1st Edn., Société des Electrodes Réfractaires Savoie (1981).
3. Brown, F. J., Palmer, J. D., Wood, P.: Nucl. Graph. Waste Manage. IAEA **10**, 1 (1999).
4. Colle, C., Adam, C.: Fiche Radionucléide IRSN (2002).
5. Toulhoat, P.: Scientific bases for nuclear waste management XXX. Mat. Res. Soc. Symp. Proc. **985**, 0985-NN07-02 (2007).
6. Sheppard, S. C., Johnson, L. H., Goodwin, B. W., Tait, J. C., Wuschke, D. M.: Waste Manage. **16**, 607 (1996).
7. Amiro, B. D., Sheppard, S. C., Johnston, F. L., Evenden, W. G., Harris, D. R.: Sci. Total Environ. **187**, 93 (1996).
8. Wright, J.: *Gas Chemistry in Nuclear Reactors and Large Industrial Plant, Proceedings of Salford*. 1st Edn., A. Dyer, London (1980).
9. Vaudey, C. E., Toulhoat, N., Moncoffre, N., Bérerd, N., Raimbault, L., Sainsot, P., Rouzaud, J. N., Perrat-Mabilon, A.: J. Nucl. Mater. **395**, 62 (2009).
10. Clayton, A. M., Harper, A., Wheatley, C. J.: AEA Technology, Behaviour of chlorine in nuclear graphites. UK NIREX report T/REP/20121/P/04, 4th Edn. (1996).

11. Thomsen, V., Schatzlein, D., Mercuro, D.: Spectroscopy **18**, 112 (2003).
12. Polovina, M., Babic, B., Kaluderovic, B., Dekanski, A.: Carbon **35**, 1047 (1997).
13. Takeda, M., Ueda, A., Hashimoto, H., Yamada, T., Suzuki, N., Sato, M., Tsubouchi, N., Nakazato, Y., Ohtsuka, Y.: Fuel **85**, 235 (2006).
14. Estrade-Szwarckopf, H.: Carbon **42**, 1713 (2004).
15. van Attekum, P. M. Th. M., Wertheim, G. K.: Phys. Rev. Lett. **43**, 1896 (1979).
16. Sette, F., Wertheim, G. K., Ma, Y., Meigs, G., Modesti, S., Chen, C. T.: Phys. Rev. **41**, 9766 (1990).
17. Speranza, G., Minati, L., Anderle, M.: J. Appl. Phys. **102**, 043504-1 (2007).
18. Lee, W. H., Kim, S. J., Lee, W. J., Lee, J. G., Haddon, R. C., Reucroft, P. J.: Appl. Surf. Sci. **181**, 121 (2001).
19. Moulder, J., Stickle, W. F., Sobol, P. E., Bomben, K. D.: *Handbook of X-Ray Photoelectron Spectroscopy*. 2nd Edn., Perkin Elmer Corporation, Eden Prairie, MN (1992).
20. Papirer, E., Lacroix, R., Donnet, J. B., Nansé, G., Fioux, P.: Carbon **33**, 63 (1995).
21. Lee, W. H., Kim, S. J., Lee, W. J., Lee, J. G., Haddon, R. C., Reucroft, P. J.: Appl. Surf. Sci. **181**, 121 (2001).
22. Pérez-Cadenas, A. F., Maldonado-Hodar, F. J., Moreno-Castilla, C.: Carbon **41**, 473 (2003).
23. Gonzalez, J., del C. Ruiz, M., Bohé, A., Pasquevich, D.: Carbon **37**, 1979 (1999).
24. Hering, H.: *Génie Atomique Tome V: Elaboration des Matériaux Nucléaires de Base. Elaboration et Utilisation des Éléments Artificiels. Chapitre XIII: Production des Graphites Pour Usages Nucléaires*. 2nd Edn., INSTN, Saclay (1965).
25. Barrie, A., Drummond, I. W., Herd, Q. C.: J. Electron Spectrosc. Relat. Phenom. **5**, 217 (1974).
26. Comte, J.: Lixiviation des poudres d'empilements de graphite de Bugey. CEA analytical report SA3C/LARC 2004/0329 (2006).
27. Guy, C., Comte, J., Combes, C., Senes, S., Thouvenin, M.: Lixiviation des empilements graphite de G2, comportement des radio-nucléides. 1st Edn., CEA technical note SA3C/LARC 07-02 (2007).
28. Pichon, C.: Comportement des radionucléides dans les graphites UNGG en milieu aqueux. 1st Edn., CEA technical note SA3C/LARC 08-02 (2008).